Supporting information to:

Time-resolved observation of protein allosteric communication

Sebastian Buchenberg, Florian Sittel and Gerhard Stock[1]

Biomolecular Dynamics, Institute of Physics,
Albert Ludwigs University, 79104 Freiburg, Germany

E-mail: stock@physik.uni-freiburg.de

April 26, 2017

[1] To whom correspondence should be addressed

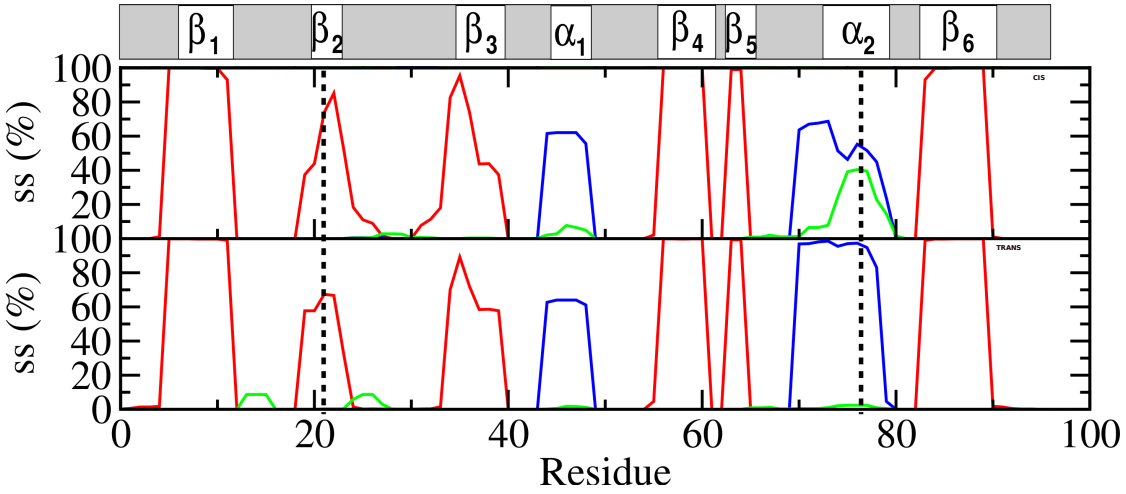

FIG. S1: Secondary structure content of PDZ2S in (top) *cis* and (bottom) *trans* state for the equilibrium MD simulations. The content of β-sheet (red), α-helical (blue) and 3_{10}-helical conformations of the individual residues are shown obtained by DSSP (W. Kabsch and C. Sander, Biopolymers 22, 2577-2637 (1983)).

S_i	S_j	i	j	ΔP	type
α_2	α_2	Gln-73	Thr-77	0.31	HB_{mc}
α_2	α_2	Ala-74	Leu-78	0.41	HB_{mc}
α_2	α_2	Val-75	Arg-79	0.40	HB_{mc}
α_2	α_2	Val-75	Leu-78	-0.42	HB_{mc}
α_2	β_1-β_2	Cys-76	Ser-17	-0.34	–
α_2	β_1-β_2	Leu-78	Lys-13	-0.40	–
α_2	β_1-β_2	Leu-78	Leu-18	-0.39	np
α_2	β_2	Val-75	Val-22	-0.32	np
α_2	β_2	Arg-79	Cys-21	0.64	–
α_2	β_3	Ala-74	Ile-35	0.37	np
α_2	β_3	Leu-78	Ile-35	0.50	np
α_2	β_5	Thr-77	Val-64	0.31	–
α_2	β_6	Leu-78	Val-85	-0.33	np
α_2	β_5-α_2	Gln-73	Ala-69	0.35	–
α_2	β_5-α_2	Ala-74	Ala-69	0.30	np
α_2	β_5-α_2	Val-75	Leu-66	-0.34	np
α_2	β_5-α_2	Thr-77	Leu-66	0.50	–
β_5-α_2	β_5	Gly-68	Ser-65	0.41	HB_{sc}
β_6	C	Glu-90	Gln-93	0.38	–
β_1-β_2	β_1-β_2	Lys-13	Asp-15	-0.38	–
β_1-β_2	β_1-β_2	Lys-13	Ser-17	0.32	–
β_1-β_2	β_1-β_2	Asn-14	Ser-17	0.42	HB_{mc}
β_1-β_2	α_2-β_6	Asn-14	Gln-83	-0.40	–
β_2-β_3	β_2-β_3	Gly-24	Gly-34	-0.32	–
β_2-β_3	β_5-α_2	His-32	Glu-67	0.32	–
β_2-β_3	C	Val-30	Ser-94	0.38	–
β_2-β_3	C	Val-30	Pro-95	0.31	–
β_3	β_5-α_2	Ile-35	Ala-69	-0.41	np
β_3	β_5-α_2	Ile-35	Thr-70	-0.39	–
β_3	C	Tyr-36	Ser-94	0.43	–
α_1-β_4	C	Gly-55	Gln-93	0.34	–
α_1-β_4	C	Gly-55	Ser-94	0.44	–
β_4	β_5-α_2	Arg-57	Glu-67	0.34	–
β_4	α_2-β_6	Val-61	Thr-81	0.35	–

TABLE S1: Contacts between residue i in segment S_i and residue j in segment S_j that change significantly ($\Delta P_{ij} \geq 0.3$) upon *cis-trans* isomerization of PDZ2S, where $\Delta P_{ij} = P_{ij}^{\text{trans}} - P_{ij}^{\text{cis}}$ denotes the change of the contact probability. Here P_{ij}^{cis} or P_{ij}^{trans} denote the probability that the minimal distance between residue i and j in PDZ2S-cis or -trans, respectively, is below 0.45 nm. The last column indicates whether a given contact is a H bond within the main chain (HB_{mc}), a H bond between the main and a side chain (HB_{sc}), or a contact between two hydrophobic residues (np). In line with the discussion, the upper part of the table describes contact changes at the α_2 side and the lower part changes at the β_2 side of the binding pocket.

Residue	rmsd(nm)	Region	*cis*	*trans*	$\Delta d_{i-1,i+1}$ (nm)	s
Gly-4	0.010	N	δ'	δ', P_{II}, ϵ	0.0144($\pm$0.0100)	1
Lys-13	0.016		β, P_{II}, ζ, δ'	P_{II}	0.0052($\pm$0.016)	0
Asn-14	0.040		P_{II}, α, P'_{II}, (β)	β, (P_{II}, α)	0.034($\pm$0.016)	1
Asp-15	0.042	$\beta_1 - \beta_2$	α, β, γ, δ	δ'	$-$0.065($\pm$0.017)	-1
Asn-16	0.053		α, β, P_{II}, δ, δ'	δ', α	$-$0.077($\pm$0.013)	-1
Gly-19	0.0094		δ', P'_{II}	δ'	$-$0.009($\pm$0.013)	0
Gly-25	0.027		β, P_{II}, α, P'_{II}, ϵ, δ'	P_{II}, (P'_{II}, ϵ)	$-$0.053($\pm$0.023)	-1
Val-26	0.016		β, P_{II}, (α)	β, P_{II}, δ', (α)	$-$0.024($\pm$0.016)	-1
Asn-27	0.016		P_{II}, α, δ	δ', (β, P_{II})	$-$0.005($\pm$0.024)	0
Thr-28	0.013	$\beta_2 - \beta_3$	β, P_{II}, α	β, (P_{II}, α, δ')	0.020($\pm$0.025)	0
Ser-29	0.023		α, δ', (P_{II})	α, δ', P_{II}	0.016($\pm$0.018)	0
Arg-31	0.015		α, δ', (P_{II})	β, δ', α, γ	0.017($\pm$0.021)	0
Gly-33	0.029		P_{II}, ϵ, α, δ', P'_{II}	P_{II}, ϵ, α, δ', P'_{II}, (ϵ)	$-$0.038($\pm$0.020)	-1
Gly-34	0.014		P_{II}, P'_{II}, ϵ	P_{II}, P'_{II}, (ϵ)	$-$0.0111($\pm$0.0076)	-1
Lys-54	0.013	$\alpha_1 - \beta_4$	P_{II}, α	P_{II}, (α)	0.0156($\pm$0.0078)	1
Leu-66	0.011		α, (β)	α	$-$0.0156($\pm$0.0038)	-1
Glu-67	0.024		P_{II}, α	α, (P_{II})	$-$0.026($\pm$0.014)	-1
Gly-68	0.025	$\beta_5 - \alpha_2$	α, δ', γ	α, δ', (γ)	$-$0.029($\pm$0.014)	-1
Ala-69	0.020		β, P_{II}, (α)	β, P_{II}	0.036($\pm$0.015)	1
Thr-70	0.027		P_{II}, α, δ'	P_{II}	0.023($\pm$0.013)	1
His-71	0.012		α, (β, P_{II})	α	$-$0.015($\pm$0.017)	0
Cys-76	0.0098	α_2	δ, α	α	$-$0.0005($\pm$0.0025)	0
Asn-80	0.017		α, γ'	γ', (α, β)	$-$0.01085($\pm$0.0050)	-1
Gly-92	0.030	C	P_{II}, (P'_{II})	P_{II}, α', δ'	$-$0.0412($\pm$0.014)	-1

TABLE S2: Residues i showing large changes in their main chain conformations between *cis* and *trans* state and extent of changes. The latter is quantified in terms of the rmsd between the average structures of the residues in the *cis* and *trans* state. Only residues with rmsd values above 0.085 nm are listed. Corresponding motifs in the *cis* and *trans* state are given in the nomenclature proposed by Hollingsworth and Karplus (Bioimol. Concepts 1, 271-283 (2010)). Brackets indicate motifs that are only weakly populated. In addition, changes in the C_α distances between corresponding neigboring residues $i-1$ and $i+1$, $\Delta d_{i-1,i+1}$, are given. The rightmost column, s, indicates whether the changes are within the statistical error ($s = 0$), or, if not, indicating that residue i is a hinge residue, it yields the sign of $\Delta d_{i-1,i+1}$. Thus, $s < 0$ or $s > 0$ means that the C_α distance between residues $i - 1$ and $i + 1$ is reduced or increased, respectively.

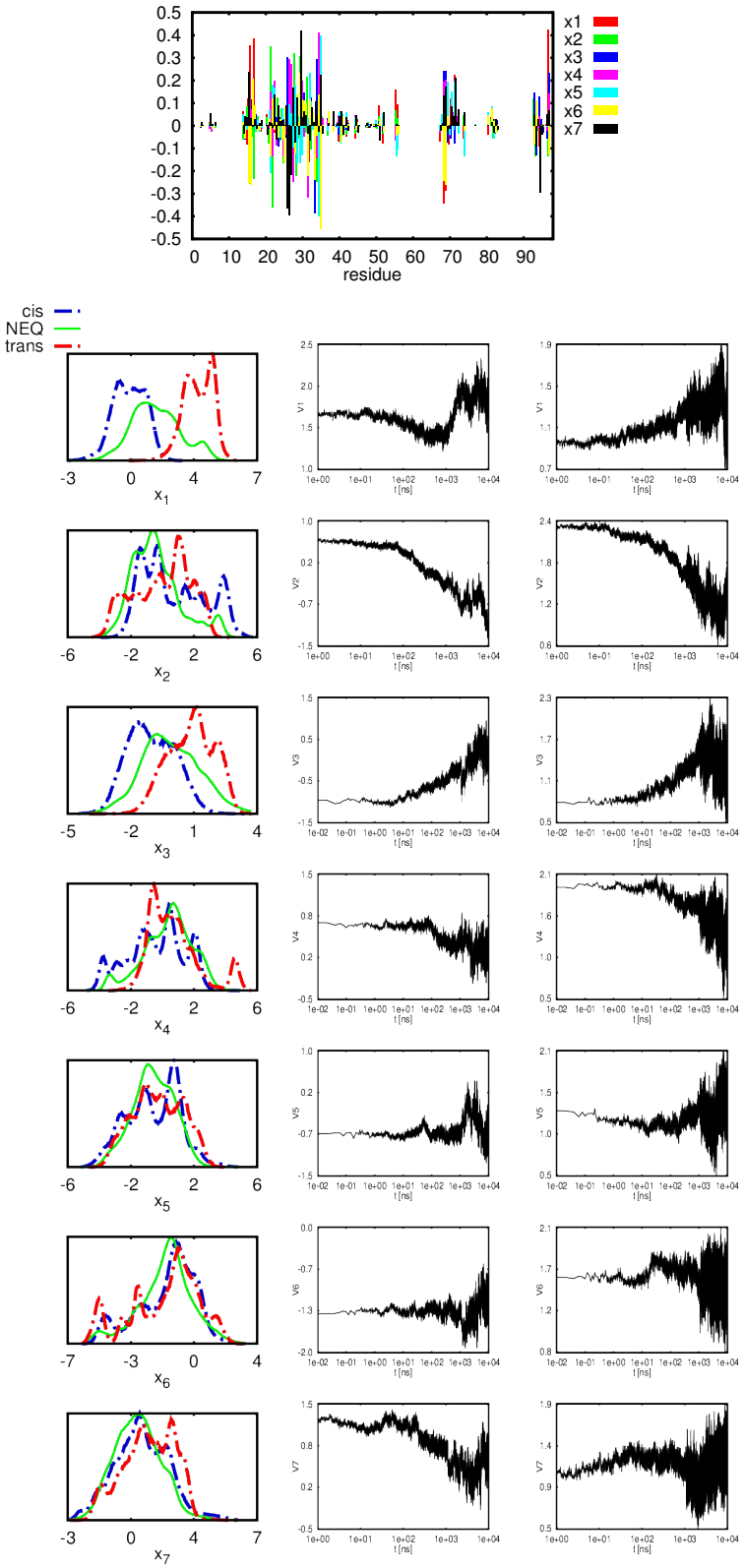

FIG. S2: (Top) Influence of the 95 preselected dihedral angles on the first seven eigenvectors of dPCA+ (see Methods section of main text). (Bottom) Distributions and time traces of the means and variances of principal components $x_1 - x_7$.

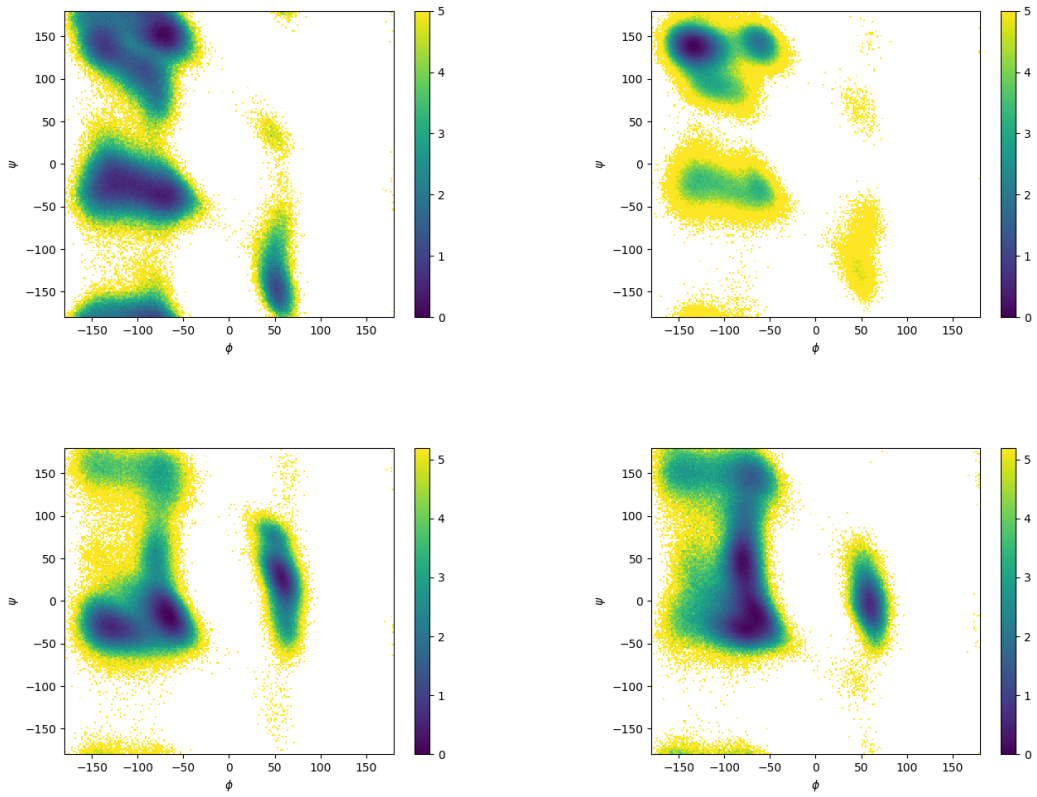

FIG. S3: Ramachandran plots of (top left) Asn_{14} in *cis*, (top right) Asn_{14} in *trans*, (bottom left) Ser_{29} in *cis*, and (bottom right) Ser_{29} in *trans* configuration.

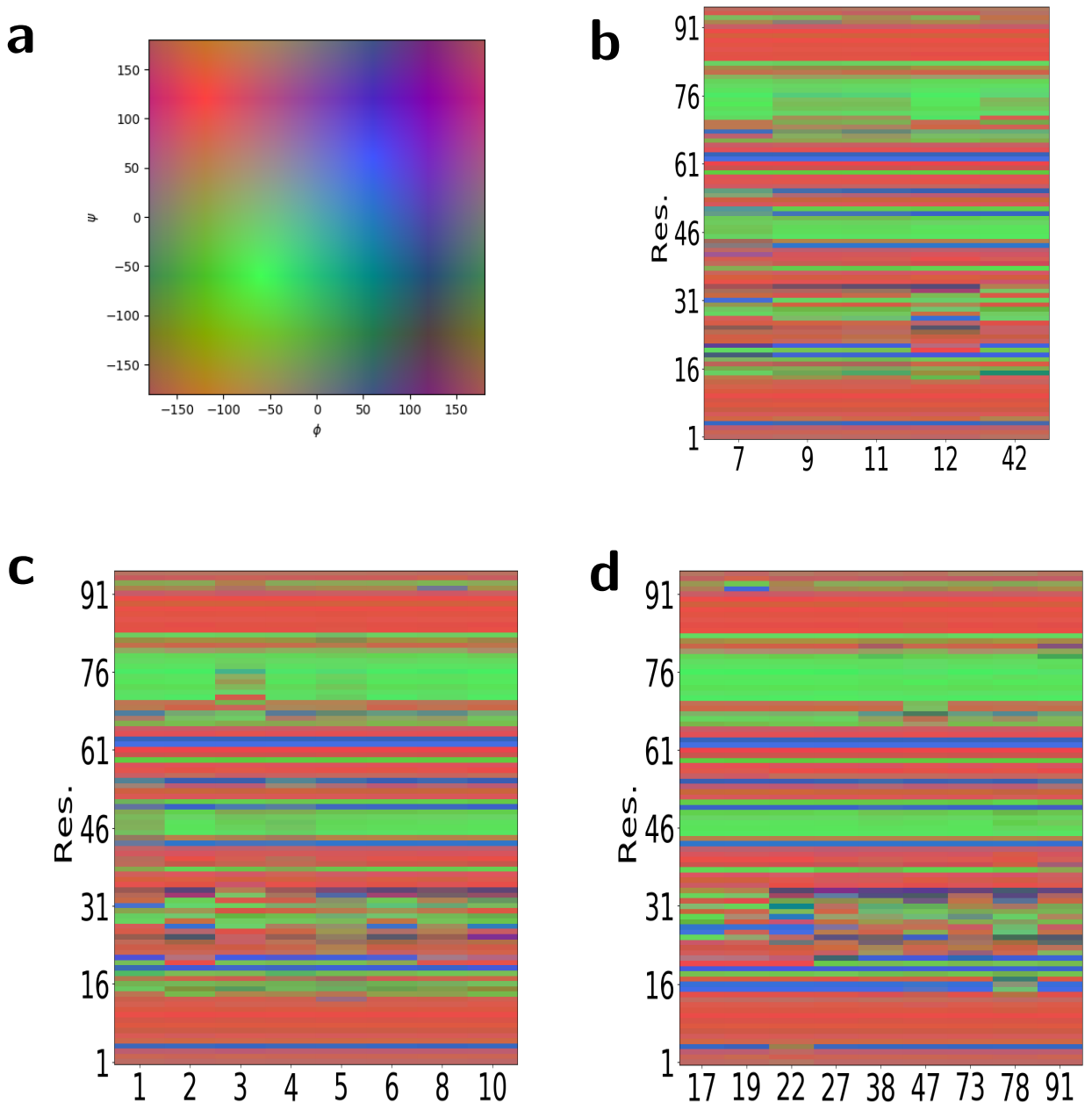

FIG. S4: Ramacolor plots (F. Sittel and G. Stock, J. Chem. Theory Comp. 12, 2426-2435 (2016)) for selected *cis* (b), NEQ (c), and *trans* (d) microstates. As displayed by the ϕ, ψ color space in (a), the plots give an impression of the structural differences of states and their respective secondary structure content. The x-axis gives the state while the y-axis denotes the index of a residue. The colors of the boxes are computed from the color code weighted by the intra state distribution in the Ramachandran plot. The typical secondary structure elements are highlighted by green (α-helix), red (β-sheet) and blue (left-handed α-helix).

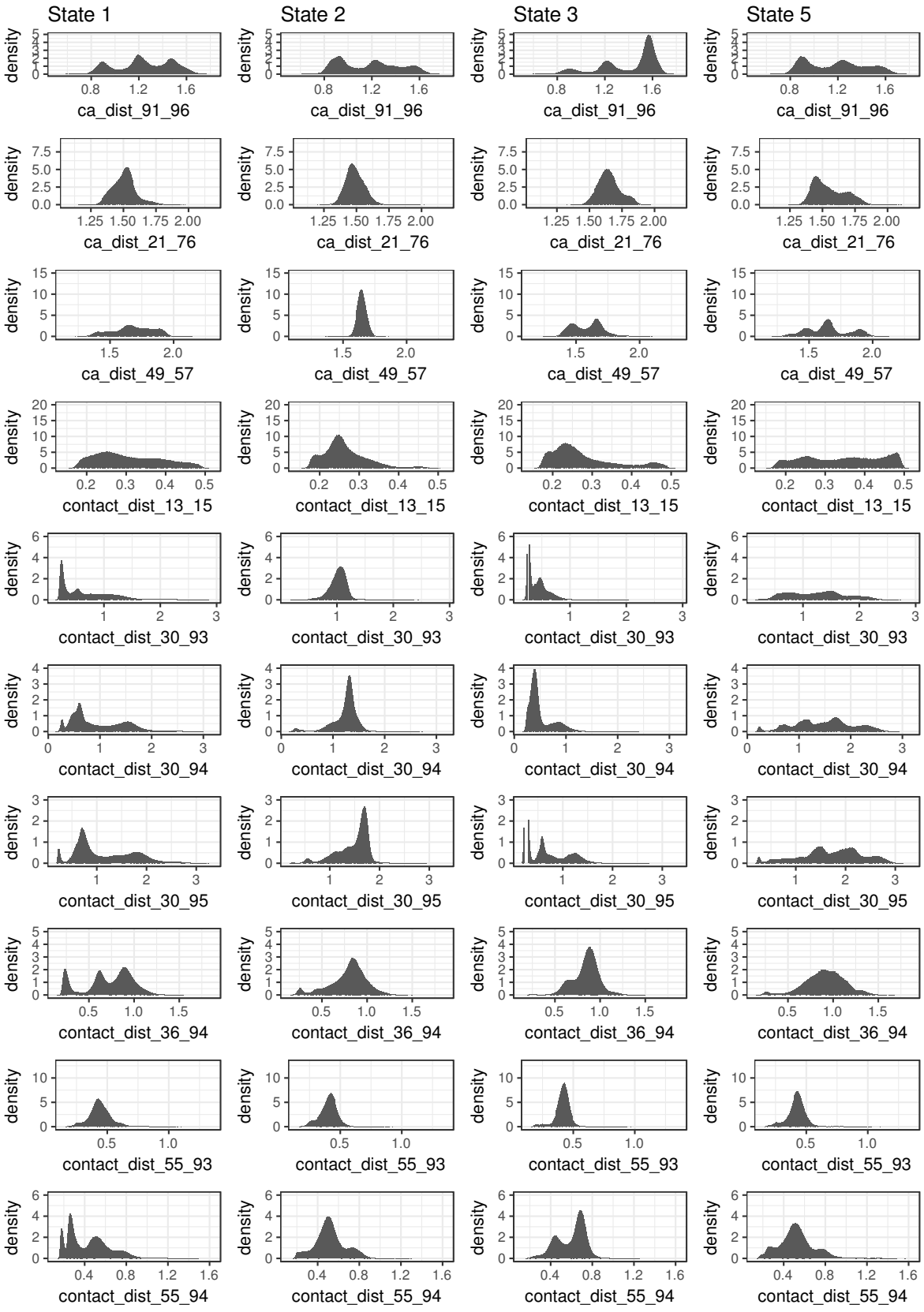

FIG. S5: Distance distributions (in units of nm) of selected microstates (1 of 2).

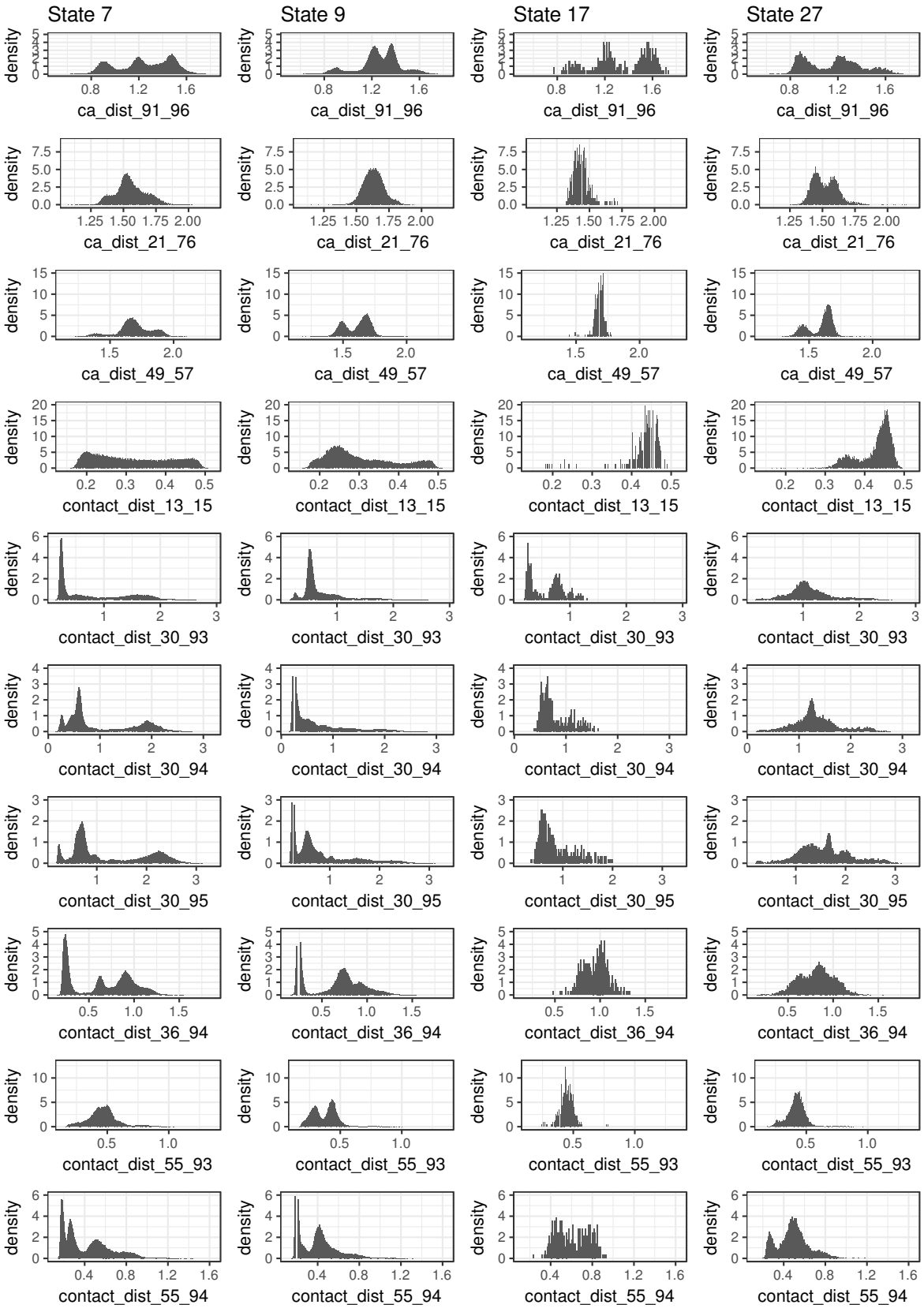

FIG. S5: Distance distributions (in units of nm) of selected microstates (2 of 2).

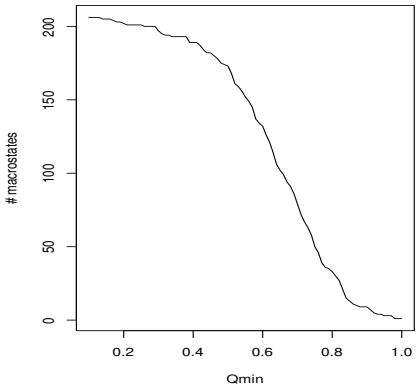

FIG. S6: Number of macrostates as a function of the metastability $Q_{\min}$ using a lag time of $\tau = 1$ ns. The macrostates are based on dynamical clustering using the Most Probable Path method by A. Jain and G. Stock (J. Chem. Theory Comp. 8, 3810-3819 (2012)).

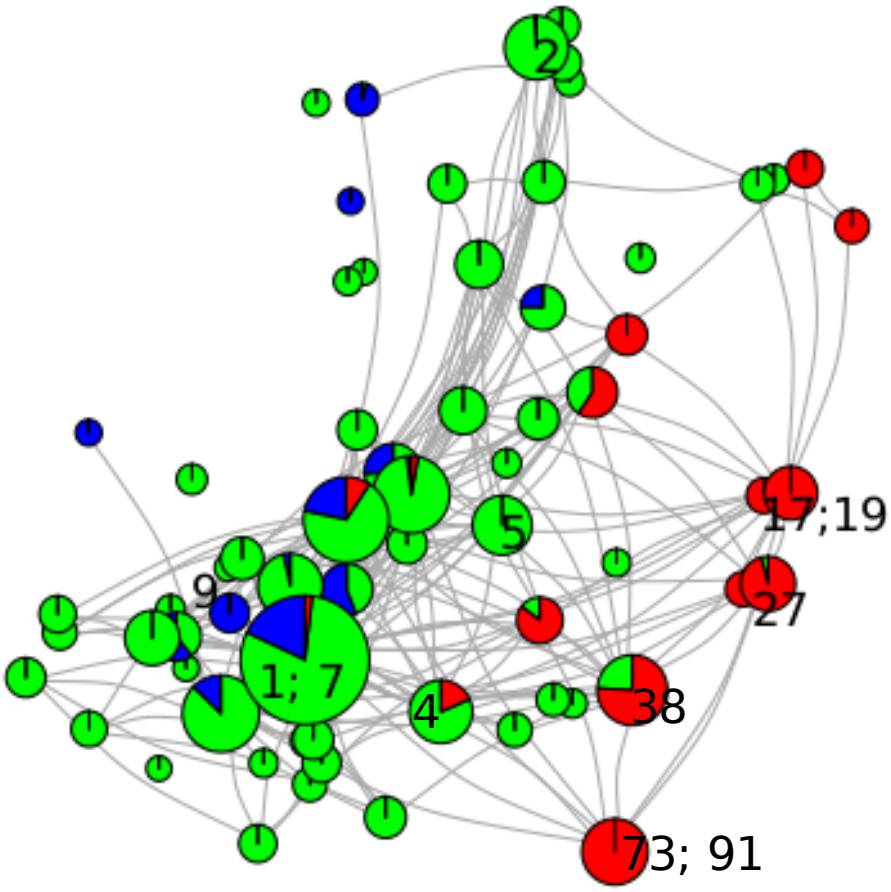

FIG. S7: Dynamical network of macrostates obtained for $Q_{\min} = 0.72$, placing the states according to their position in x_1-x_2 space. Nodes are colored by their respective content of microstates identified as *cis* (blue), NEQ (green) or *trans* (red). Selected microstates are labeled at the macrostate they are part of. As in Fig. S6, the macrostates and connections are based on dynamical clustering using the Most Probable Path method.